Capture process in nuclear reactions with a quantum master equation

V. V. Sargsyan,[1,2] Z. Kanokov,[1,3] G. G. Adamian,[1,4] N. V. Antonenko,[1] and W. Scheid[5]

[1]*Joint Institute for Nuclear Research, RU-141980 Dubna, Russia*

[2]*Yerevan State University, 0025 Yerevan, Armenia*

[3]*National University, 700174 Tashkent, Uzbekistan*

[4]*Institute of Nuclear Physics, 702132 Tashkent, Uzbekistan*

[5]*Institute für Theoretische Physik der Justus-Liebig Universität, D-35392 Giessen, Germany*

(Received 20 May 2009; published 10 September 2009)

Projectile-nucleus capture by a target nucleus at bombarding energies in the vicinity of the Coulomb barrier is treated with the reduced-density-matrix formalism. The effects of dissipation and fluctuations on the capture process are taken self-consistently into account within the quantum model suggested. The excitation functions for the capture in the reactions ^{16}O, ^{19}F, ^{26}Mg, ^{28}Si, ^{32,34,36,38}S, ^{40,48}Ca, ^{50}Ti, ^{52}Cr + ^{208}Pb with spherical nuclei are calculated and compared with the experimental data. At bombarding energies about (15–25) MeV above the Coulomb barrier the maximum of capture cross section is revealed for the ^{58}Ni + ^{208}Pb reaction.

DOI: 10.1103/PhysRevC.80.034606 PACS number(s): 25.70.Jj, 24.10.−i, 24.60.−k

I. INTRODUCTION

The dynamics of interaction between two heavy ions at bombarding energies in the vicinity of the Coulomb barrier has been the subject of intensive theoretical and experimental investigations [1–13]. In recent years, these investigations have been motivated by successes of the synthesis of new superheavy elements in cold- and hot-fusion reactions [7–9]. The process of projectile-nucleus capture by a target nucleus is an important stage of fusion reactions. At energies near the Coulomb barrier, the evaporation residue cross sections crucially depend on the capture cross sections. The classical deterministic Newton equation with a friction force for the relative distance between the centers of mass of colliding nuclei has been often used to describe the capture process [6]. The diffusion Fokker-Planck equation and the stochastic Langevin equation have been also used to describe this process [2,3,14].

Many studies based on the transport models ignore the quantum-mechanical statistical effects and employ a classical description where the coefficient of friction is related to the diffusion coefficient by the classical fluctuation-dissipation relation. The description of fluctuations and dissipation is usually restricted to the Markov limit even in the case of low temperatures and strong coupling between the collective and internal subsystems for the processes as fast as heavy-ion collisions [15]. So far, no model that would take into account all quantum-mechanical effects and non-Markovian effects accompanying the passage through the potential barrier has been developed. Because the Coulomb barrier frequency is higher than the temperature of a dinuclear system at the instant of its formation, the quantum fluctuations about the mean value of the trajectory of colliding nuclei may affect the evaporation residue cross section through the capture probability. It should be noted that the passage through the Coulomb barrier approximated by a parabola has been previously studied in the Refs. [15–18].

The objective of the present study is to include the quantum-mechanical fluctuation and dissipation effects in the description of the capture process within the reduced-density-matrix formalism [16]. The non-Markovian quantum diffusion coefficients are used in the master equation for the density matrix. With the aid of the proposed quantum-mechanical formalism we study the capture probability as a function of the potential pocket depth, collision energy, and magnitude of angular momentum. The respective calculations are used to determine the capture cross sections in asymmetric fusion reactions with spherical nuclei at energies near the Coulomb barrier and higher. The results obtained in this way are compared with the available experimental data. New experiments are suggested to observe the interesting phenomena in the capture process.

II. MASTER EQUATION FOR THE REDUCED DENSITY MATRIX

The effect of internal degrees of freedom on the evolution of a quantum-mechanical system along the collective coordinate R (the relative distance between the centers of mass of interacting nuclei) can be described in terms of the reduced density matrix. The reduced density matrix ρ for the collective subsystem satisfies the equation [19–23]:

$$\frac{d}{dt}\rho = -\frac{i}{\hbar}[H_c,\rho] - \frac{i\lambda_P}{2\hbar}[R,\{P,\rho\}_+] - \frac{D_{PP}}{\hbar^2}[R,[R,\rho]] + \frac{D_{RP}}{\hbar^2}[P,[R,\rho]] + [R,[P,\rho]]\frac{D_{RP}}{\hbar^2}, \quad (1)$$

where $H_c = \frac{1}{2\mu}P^2 + V$ is the collective Hamiltonian of the radial motion and μ is the reduced mass. The potential V is the renormalized (because of the coupling to internal degrees of freedom) collective potential; D_{PP}, D_{RP}, and λ_P are, respectively, the coefficient of diffusion in momentum, the mixed diffusion coefficient, and the coefficient of friction. If the coupling between the collective and internal subsystems

is in the coordinate, the coefficients of diffusion and friction in coordinate vanish [16]. Based on the results of Ref. [23], the asymptotic values of friction and diffusion coefficients are used in Eq. (1).

The friction coefficient λ_P depends on R for the coupling type being considered. We use a well-known phenomenological formula [1,2]

$$\lambda_P(R) = \alpha \left| \frac{\partial}{\partial R} V_{\rm nuc}(R) \right|^2, \tag{2}$$

where $V_{\rm nuc}(R)$ is the nuclear part of the nucleus-nucleus potential V and the parameter α is a constant to fix the certain value of $\lambda_P(R_b)$ on the top of the Coulomb barrier at $R = R_b$.

If the potential V is an oscillator potential and if the coupling of the collective subsystem to the internal subsystem is linear in R, then the diffusion coefficients in Eq. (1) are independent of R [16,21,22]. In this case, D_{PP} and D_{RP} are functions of the oscillator frequency [16]. By means of an expansion in a Taylor series to the second-order inclusive, one can approximate a more complicated potential V at each point R by a local harmonic or inverted oscillator. Because the local-oscillator frequency

$$\omega(R) = \sqrt{\frac{1}{\mu} \left| \frac{\partial^2 V}{\partial R^2} \right|}$$

and friction coefficient $\lambda_p(R)$ depend on the coordinate, the asymptotic diffusion coefficients (see Appendix)

$$D_{PP} = \frac{T\mu\gamma^2\lambda_P}{\gamma(\gamma+\lambda_P) \pm \omega^2} \times \left\{ 1 + 2\sum_{k=1}^{\infty} \frac{\nu_k\gamma\lambda_P \pm \omega^2(\gamma+\nu_k)}{(\gamma+\nu_k)[\nu_k(\nu_k+\lambda_P) \pm \omega^2]} \right\}, \tag{3}$$

$$D_{RP} = \frac{T\gamma\lambda_P}{2[\gamma(\gamma+\lambda_P) \pm \omega^2]} \times \left\{ 1 + 2\gamma\sum_{k=1}^{\infty} \frac{-\nu_k\gamma \pm \omega^2}{(\gamma+\nu_k)[\nu_k(\nu_k+\lambda_P) \pm \omega^2]} \right\} \tag{4}$$

also become coordinate-dependent quantities [23]. Here, $\nu_k = 2\pi T k/\hbar, T$ is the temperature of the internal subsystem, and the upper and lower signs refer to a harmonic and an inverted oscillators, respectively. Non-Markovian effects appear in the diffusion coefficients and, accordingly, in the master Eq. (1) through the internal-excitation width of $\hbar\gamma = 12$ MeV. The relaxation time for the internal subsystem is much shorter than the characteristic time of collective motion. For an anharmonic potential V, the use of independent of R diffusion coefficients seems to be a good approximation only in the case of a weak dissipation and high temperature [19,21,22]. However, in many applications, for example, in the decay from a moderately shallow potential well, one should take into account higher-order fluctuations [23]. The use of asymptotic diffusion coefficients in our calculations is well justified because the interaction between two nuclei starts well before the Coulomb barrier and these asymptotics are established for the underdamped motion in R much faster than the capture occurs.

Rewriting Eq. (1) for the reduced density matrix ρ in the coordinate representation ($\rho(t,x,y) = \langle x|\rho|y\rangle$), transforming the coordinates as $x = R + z/2$ and $y = R - z/2$, and expanding the potential in z to the third-order terms inclusive, we reduce the equation for the density matrix $\rho(t,R,z)$ [23] to the form

$$\frac{d}{dt}\rho(t,R,z) = L(R,z)\rho(t,R,z),$$
$$L(R,z) = i\frac{\hbar}{\mu}\frac{\partial^2}{\partial R\partial z} - iz\frac{\partial V}{\partial R} - i\frac{1}{24}z^3\frac{\partial^3 V}{\partial R^3} - \lambda_P z\frac{\partial}{\partial z} - \frac{D_{PP}}{\hbar^2}z^2 - \frac{i}{\hbar}\left(zD_{RP}\frac{\partial}{\partial R} + \frac{\partial}{\partial R}zD_{RP} \right). \tag{5}$$

To solve Eq. (5) numerically, we use a harmonic-oscillator basis:

$$\rho(t,R,z) = \sum_{k=0}^{n} f_k(t,R)B_k(\sigma,z),$$
$$B_k(\sigma,z) = \frac{i^k}{k!}\left(\frac{k}{2}\right)! e^{-\frac{z^2}{8\sigma^2}} H_k\left(\frac{z}{2\sigma}\right). \tag{6}$$

Here, $B_k(\sigma,0) = 1$ and 0 for, respectively, even and odd values of k. We found that the diffusion coefficient D_{PP} in the minimum of the potential, to which the capture is treated, and the optimal basis parameter σ are related: $4\sigma^2 D_{PP} = \hbar^2\lambda_P$. The proposed method makes it possible to obtain ρ for a potential of any degree of intricacy and for any set of coefficients of friction and diffusion. The microscopic diffusion coefficients used ensure that the density matrix is positive at any instant and that

$$\mathrm{Tr}\rho = \sum_{k=0,2,4,\ldots} \int_{-\infty}^{\infty} f_k(t,R)dR = 1. \tag{7}$$

III. CAPTURE PROCESS

The potential describing the interaction of two nuclei can be represented in the form

$$V(R,L) = V_{\rm nuc}(R) + V_{\rm Coul}(R) + V_{\rm rot}(R,L), \tag{8}$$

where $V_{\rm nuc}$, $V_{\rm Coul}$, and $V_{\rm rot}$ stand for, respectively, the nuclear, the Coulomb, and the centrifugal potentials. The nuclei are proposed spherical and the potential depends on the distance R between the center of mass of two interacting nuclei and angular momentum L. For the nuclear part of the nucleus-nucleus potential, we use the double-folding formalism [24], taking it in the form

$$V_{\rm nuc} = \int \rho_1(\mathbf{r_1})\rho_2(\mathbf{R}-\mathbf{r_2})F(\mathbf{r_1}-\mathbf{r_2})d\mathbf{r_1}d\mathbf{r_2}, \tag{9}$$

where $F(\mathbf{r_1}-\mathbf{r_2}) = C_0[F_{\rm in}\frac{\rho_0(\mathbf{r_1})}{\rho_{00}} + F_{\rm ex}(1-\frac{\rho_0(\mathbf{r_1})}{\rho_{00}})]\delta(\mathbf{r_1}-\mathbf{r_2})$ is the density-depending effective nucleon-nucleon interaction and $\rho_0(\mathbf{r}) = \rho_1(\mathbf{r}) + \rho_2(\mathbf{R}-\mathbf{r})$, $F_{\rm in,ex} = f_{\rm in,ex} + f'_{\rm in,ex}\frac{(N_1-Z_1)(N_2-Z_2)}{(N_1+Z_1)(N_2+Z_2)}$, $\rho_1(\mathbf{r_1})$, N_1, Z_1 and $\rho_2(\mathbf{r_2})$, N_2, Z_2 are the nucleon densities, neutron numbers, and charge numbers of,

respectively, the projectile and the target nucleus. Our calculations were performed with the following set of parameters: $C_0 = 300$ MeV fm^3, $f_{\rm in} = 0.09$, $f_{\rm ex} = -2.59$, $f'_{\rm in} = 0.42$, $f'_{\rm ex} = 0.54$, and $\rho_{00} = 0.17$ fm^{-3}. To calculate the Coulomb and centrifugal potentials, we use the formulas

$$V_{\rm Coul} = e^2 \int \frac{\rho_1^z(\mathbf{r_1})\rho_2^z(\mathbf{R}-\mathbf{r_2})}{|\mathbf{r_1}-\mathbf{r_2}|} d\mathbf{r_1} d\mathbf{r_2} \tag{10}$$

and

$$V_{\rm rot} = \frac{\hbar^2 L(L+1)}{2\mu R^2}, \tag{11}$$

respectively. Here, ρ_1^z and ρ_2^z are the nuclear charge densities. The nuclear densities are specified in the form of the Woods-Saxon parametrization, where the nuclear radius parameter is $r_0 = 1.15$ fm and the diffuseness parameter is $a = 0.55$ fm [24]. We used $a = 0.53$ fm only for the lighter nuclei ^{16}O and ^{19}F. Figure 1 shows the nucleus-nucleus interaction potential calculated for the ^{16}O + ^{208}Pb and ^{48}Ca + ^{208}Pb systems at various values of the orbital angular momentum L. As the centrifugal part of the potential grows, the pocket depth becomes smaller, while the position of the pocket minimum moves toward the barrier at $R = R_b$. The value of R_b is approximately equal to $R_1 + R_2 + 2$ fm where R_1 and R_2 are the radii of colliding nuclei.

Here, we restrict our consideration to the one-dimensional problem of radial motion. In addition to the dissipation of kinetic energy of the radial motion there is dissipation of angular momentum, i.e., the approach of the sticking limit [1,2]. Because the dissipation of angular momentum mainly occurs behind the barrier, for simplicity, it can be disregarded to treat the passage of the Coulomb barrier. As follows from our calculations, the dissipation of orbital angular momentum causes the decrease of the value of potential $V(R)$. However, the value of $\partial V(R)/\partial R$ is only slightly changed in the reactions considered. Thus, considering the decay or reflection from the region behind the barrier, one can use the potential at fixed angular momentum for bombarding energies of interest.

One can visualize a capture as a process in which the part of the initial Gaussian wave packet that is to the right of the barrier populates the left potential pocket (see Fig. 1). The capture probability is defined with the ratio

$$P(t, E_{\rm c.m.}, L) = \frac{\int_{-\infty}^{R_b} \rho(t,R) dR}{\int_{R_b}^{\infty} \rho(t=0,R) dR} \tag{12}$$

at $t = \tau$, i.e., $P_{\rm cap}(E_{\rm c.m.}, L) = P(\tau, E_{\rm c.m.}, L)$. The value of τ determines the time of capture. When the trajectory (the mean value of the relative distance) does not cross the top of the barrier, the τ is defined as the time of returning back to starting point of the wave packet taken at $R = R_b + 1$ fm. At this R the overlap of nucleon densities is quite small and the nuclear force play a role at smaller R. For the trajectory above the Coulomb barrier, a quasi-steady-state inverse flux from the left hand potential pocket is formed in due course of time and τ is defined as the time, within which the quasi-steady-state regime sets in.

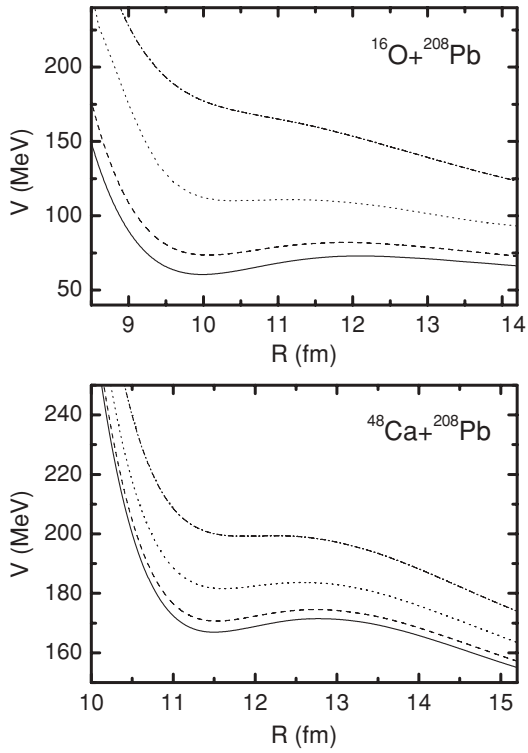

FIG. 1. Nucleus-nucleus interaction potentials as functions of the relative distance R between the centers of mass of the spherical nuclei in the ^{16}O, ^{48}Ca + ^{208}Pb reactions at various values of the orbital angular momentum $L = 0$ (solid curve), 30 (dashed curve), 60 (dotted curve), and 90 (dash-dotted curve).

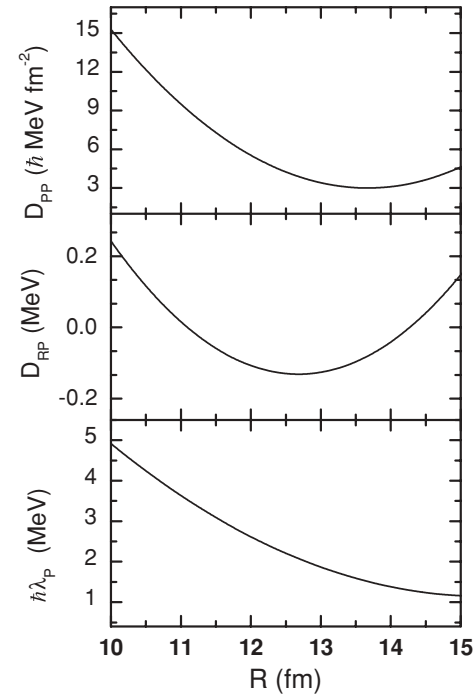

FIG. 2. Diffusion and friction coefficients versus the relative distance R at $L = 0$ for the ^{48}Ca + ^{208}Pb system whose nucleus-nucleus interaction potential is presented in Fig. 1. The parameter α is chosen from the condition $\hbar\lambda_P(R_b) = 2$ MeV.

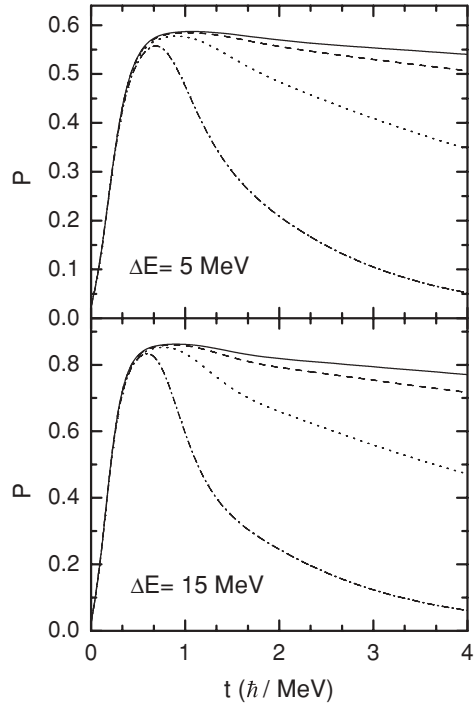

FIG. 3. The value P as a function of time at bombarding energies of $\triangle E = E_{\text{c.m.}} - V(R = R_b, L) = 5$ and 15 MeV for the $^{48}\text{Ca} + ^{208}\text{Pb}$ system. The energies $\triangle E$ are reckoned from the Coulomb barrier height at a given orbital angular momentum $L = 0$ (solid curve), 30 (dashed curve), 60 (dotted curve), and 90 (dash-dotted curve). The parameter α is chosen from the condition $\hbar\lambda_P(R_b) =$ 2 MeV.

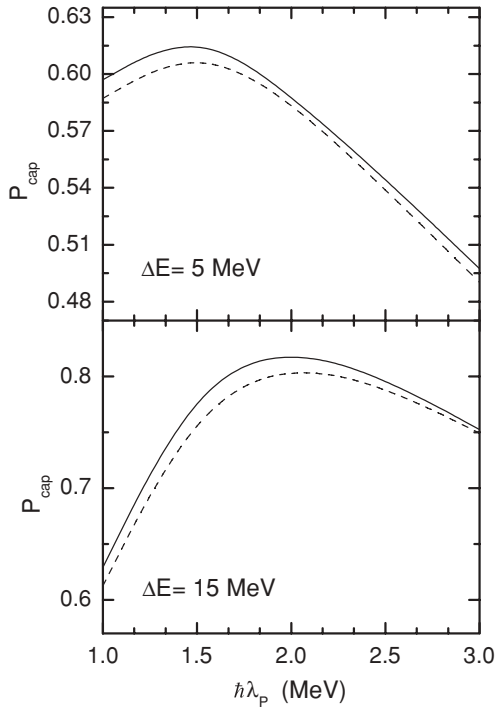

FIG. 4. Capture probability P_{cap} as a function of the friction parameter $\hbar\lambda_P(R_b)$ at indicated energies for $\hbar\gamma = 12$ MeV (solid curve) and 20 MeV (dashed curve) for the $^{48}\text{Ca} + ^{208}\text{Pb}$ reaction.

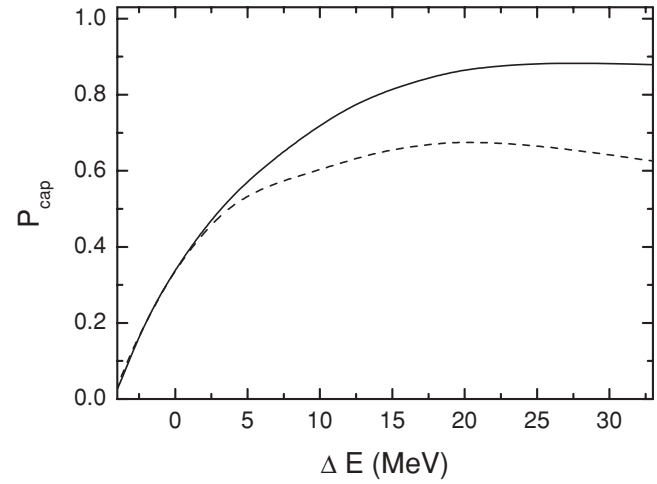

FIG. 5. Capture probability P_{cap} as a function of the bombarding energy $\triangle E = E_{\text{c.m.}} - V(R = R_b, L)$ reckoned from the Coulomb barrier height at $L = 0$ (solid curve) and 60 (dashed curve) for the $^{48}\text{Ca} + ^{208}\text{Pb}$ reaction.

The partial-wave capture cross section (cross section for the formation of a dinuclear system) is given by

$$\sigma_c(E_{\text{c.m.}}, L) = \pi\lambda\!\!\!^{-2}(2L+1)P_{\text{cap}}(E_{\text{c.m.}}, L), \tag{13}$$

where $\lambda\!\!\!^{-2} = \hbar^2/(2\mu E_{\text{c.m.}})$ is the reduced de Broglie wavelength. As follows, the total capture cross section has the form

$$\begin{aligned}\sigma_c(E_{\text{c.m.}}) &= \sum_L \sigma_c(E_{\text{c.m.}}, L) \\ &= \pi\lambda\!\!\!^{-2}\sum_L (2L+1)P_{\text{cap}}(E_{\text{c.m.}}, L).\end{aligned} \tag{14}$$

Here, the summation is in possible values of L at given $E_{\text{c.m.}}$.

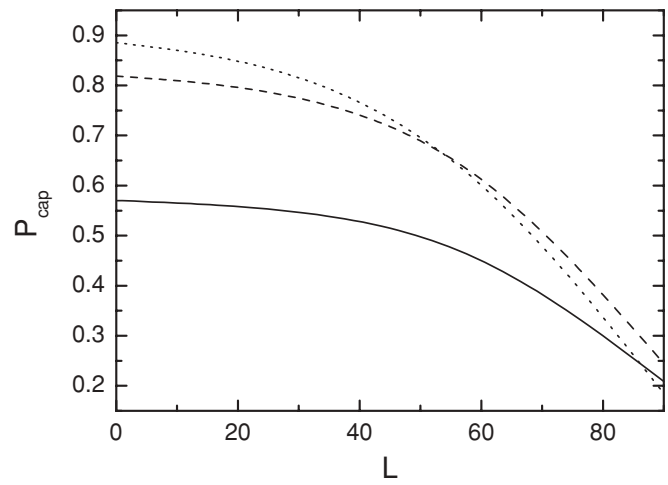

FIG. 6. Capture probability P_{cap} as a function of the orbital angular momentum at $\triangle E(0) = 5$ MeV (solid curve), 15 MeV (dashed curve), and 30 MeV (dotted curve) for the $^{48}\text{Ca} + ^{208}\text{Pb}$ reaction. The energies $\triangle E(0)$ are reckoned from the Coulomb barrier at $L = 0$.

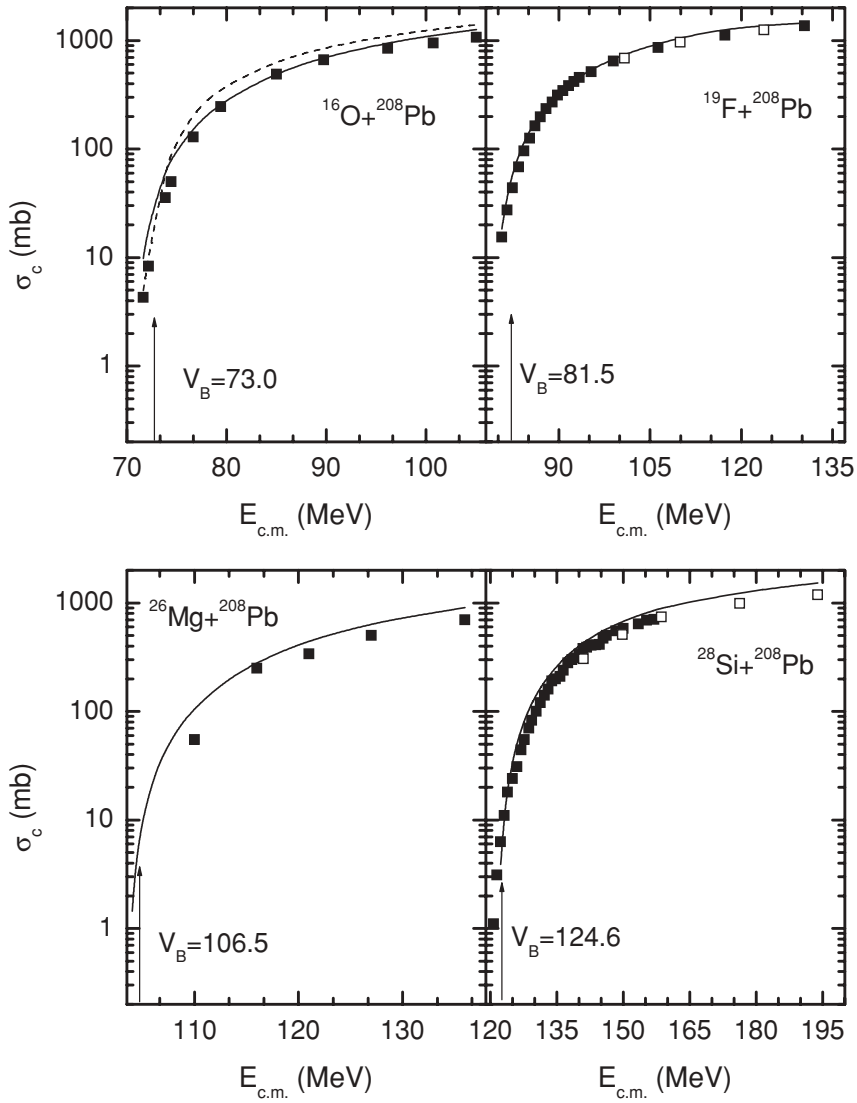

FIG. 7. Calculated capture cross sections for the indicated reactions. The experimental data for the $^{16}O + ^{208}Pb$ reaction are borrowed from Ref. [26]. The experimental data for the $^{19}F + ^{208}Pb$ reaction are borrowed from Refs. [27] (closed symbols) and [28] (open symbols). The experimental data for the $^{26}Mg + ^{208}Pb$ reaction are borrowed from Ref. [29]. The experimental data for the $^{28}Si + ^{208}Pb$ reaction are borrowed from Refs. [30] (closed symbols) and [28] (open symbols). For the $^{16}O + ^{208}Pb$ reaction, the capture cross section calculated with the Wong formula (15) is presented by dashed curve.

IV. RESULTS AND DISCUSSION

Solving the master Eq. (5), we find the diagonal elements $\rho(t, R, z = 0)$ of the density matrix in the coordinate representation. In all calculations, the Gaussian wave packet is characterized by mean coordinate $R(0) = R_b + 1.0$ fm and variances $\sigma_{RP}(0) = 0$, $\sigma_{RR}(0) = 0.25$ fm^2, and $\sigma_{PP}(0) = 1.0\hbar^2$ fm^{-2}. The mean initial momentum $P(0)$ depends on the initial energy $E_{\text{c.m.}}$.

The diffusion and friction coefficients in the master equation were calculated by formulas (2), (3), and (4). For the system $^{48}Ca + ^{208}Pb$, Fig. 2 shows the dependence of the diffusion coefficients on the coordinate R at $L = 0$ and $T = 1.2$ MeV. The coordinate dependence of the diffusion coefficients in the vicinity of the barrier is rather weak. A weak temperature dependence of the capture probability is worthy of special note [25]. A weak dependence of the diffusion coefficients on L is taken into account in our calculations. In the potential pocket region, D_{PP} and D_{RP} increases rather slowly with orbital angular momentum that is an additional argument to reduce the problem to the one-dimensional one.

Figure 3 displays the calculated time dependence of P. One can see from this figure that the time within which the quasi-steady-state flow rate sets in is $\tau \approx 2.0\hbar$/MeV. At $t > \tau$ the value of P exponentially decreases. A slump of the flux at large angular momentum ($L = 90$, dash-dotted lines) is observed because of small depth of the potential pocket. At small angular momentum the value of capture probability at $t = \tau$ is closed to the maximum value of $P(t)$ (see Fig. 3).

Figure 4 shows the capture probability P_{cap} as a function of the friction parameter $\hbar\lambda_P(R_b)$ [see Eq. (2)] at the bombarding energy values of $\triangle E(0) = E_{\text{c.m.}} - V(R = R_b, L = 0) = 5$ and 15 MeV for two different internal-excitation width $\hbar\gamma =$ 12 and 20 MeV. The dependence of P_{cap} on γ is quite weak. One can see from this figure that, as the friction becomes larger, the capture probability firstly increases but then decreases. At $\triangle E(0) = 5$ MeV (15 MeV), P_{cap} takes a maximum value at $\hbar\lambda_P(R_b) \approx 1.5$ MeV (2 MeV). This behavior is dictated by the interplay of two factors as the wave packet traverses the potential barrier. Specifically, there are friction, which impedes this process, and diffusion, which, on the contrary, facilitates

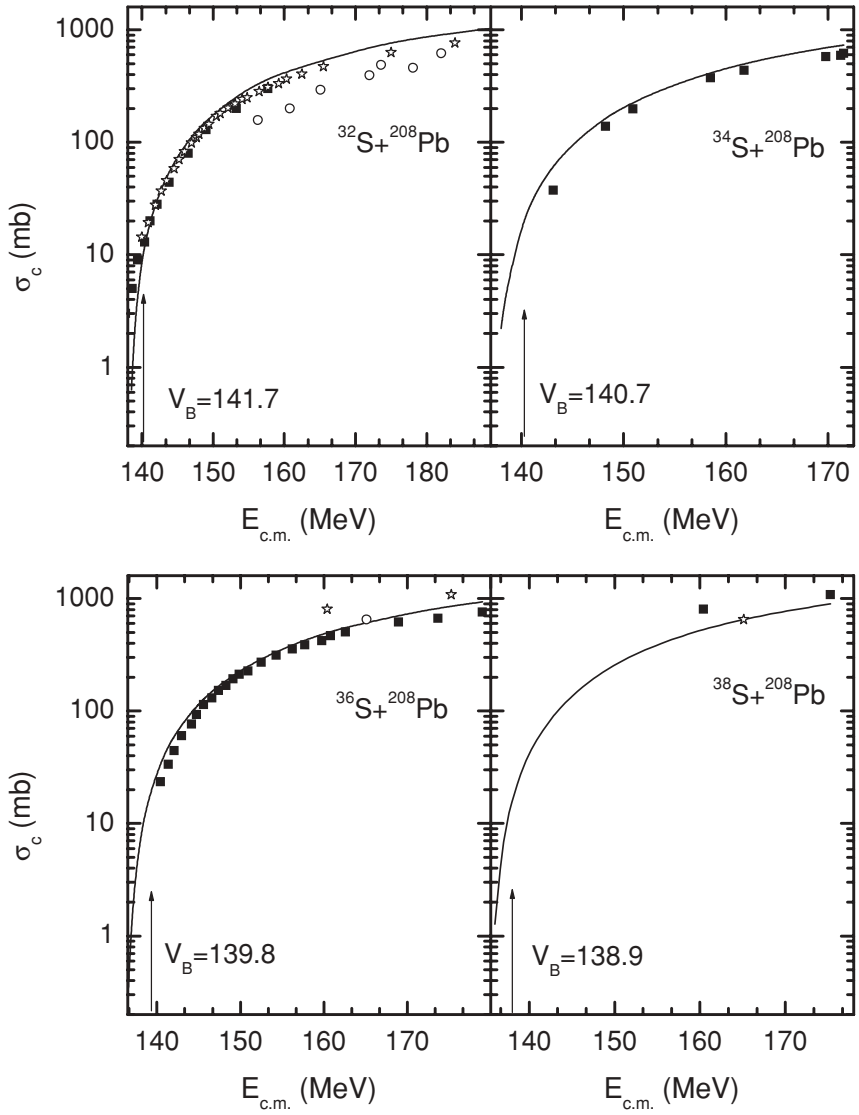

FIG. 8. Calculated capture cross sections for the indicated reactions. The experimental data for the $^{32}S + ^{208}Pb$ reaction are borrowed from Refs. [31] (closed symbols), [32] (star symbols), and [33] (circles). The experimental data for the $^{34}S + ^{208}Pb$ reaction are borrowed from Ref. [32]. The experimental data for the $^{36}S + ^{208}Pb$ reaction are borrowed from Refs. [32] (closed symbols) and [33] (star and open symbols). The experimental data for the $^{38}S + ^{208}Pb$ reaction are borrowed from Ref. [33] (closed squares and star symbols).

it. As the friction becomes larger, the diffusion grows that explains the growth of the capture probability at small friction. However, the further increasing friction leads to a decrease in the capture probability. We note that diffusion is a consequence of quantum statistical effects and vanishes in purely classical treatments of the capture process. The most realistic friction coefficients in the range of $\hbar\lambda_P \approx 1 - 2$ MeV were suggested from the study of deep inelastic reactions [5]. In this range of $\hbar\lambda_P(R_b)$ the value of $P_{\rm cap}$ is changed rather weakly, within 20%. In all our calculations below the parameter α is chosen from the condition $\hbar\lambda_P(R_b) = 2$ MeV.

Figure 5 shows the capture probability $P_{\rm cap}$ as a function of the initial bombarding energy $\triangle E = E_{\rm c.m.} - V(R = R_b, L)$ reckoned from the Coulomb barrier height at given L. The capture probability initially grows with energy, but a further increase of $\triangle E$ leads to a decrease in the probability, since, at energies considerably exceeding the barrier height, the motion of the wave packet becomes virtually free and insensitive to the presence of the potential pocket. For the angular momentum $L = 0$, the capture probability is maximal at $\triangle E \approx 30$ MeV. At $L = 60$, the maximum of $P_{\rm cap}$ is reached at $\triangle E \approx 20$ MeV. Note that, with increasing energy, the ratio $P_{\rm cap}(E_{\rm c.m.}, L = 0)/P_{\rm cap}(E_{\rm c.m.}, L = 60)$ grows, because, at the initial instant before the onset of the quasi-steady-state regime, the dissipation of energy is larger at $L = 0$ than at $L = 60$.

In Fig. 6 the capture probability $P_{\rm cap}$ is shown as a function of the orbital angular momentum at $\triangle E(0) = E_{\rm c.m.} - V(R = R_b, L = 0) = 5$, 15, and 30 MeV. With increasing L the capture probability decreases because the potential pocket becomes shallower. The rate of this decrease depends on the collision energy. Because the collective energy of the relative motion of nuclei is dissipated more vigorously with increasing initial kinetic energy, the decrease in the capture probability with increasing L is more pronounced at large positive values of $\triangle E(0)$. Note, that the dependence of $P_{\rm cap}$ on L is rather weak at $L < 60$.

The calculated capture cross sections are compared with the available experimental data [26–37] in Figs. 7–9. Our results agree well with the experimental data almost for all reactions in the large interval of bombarding energies: from

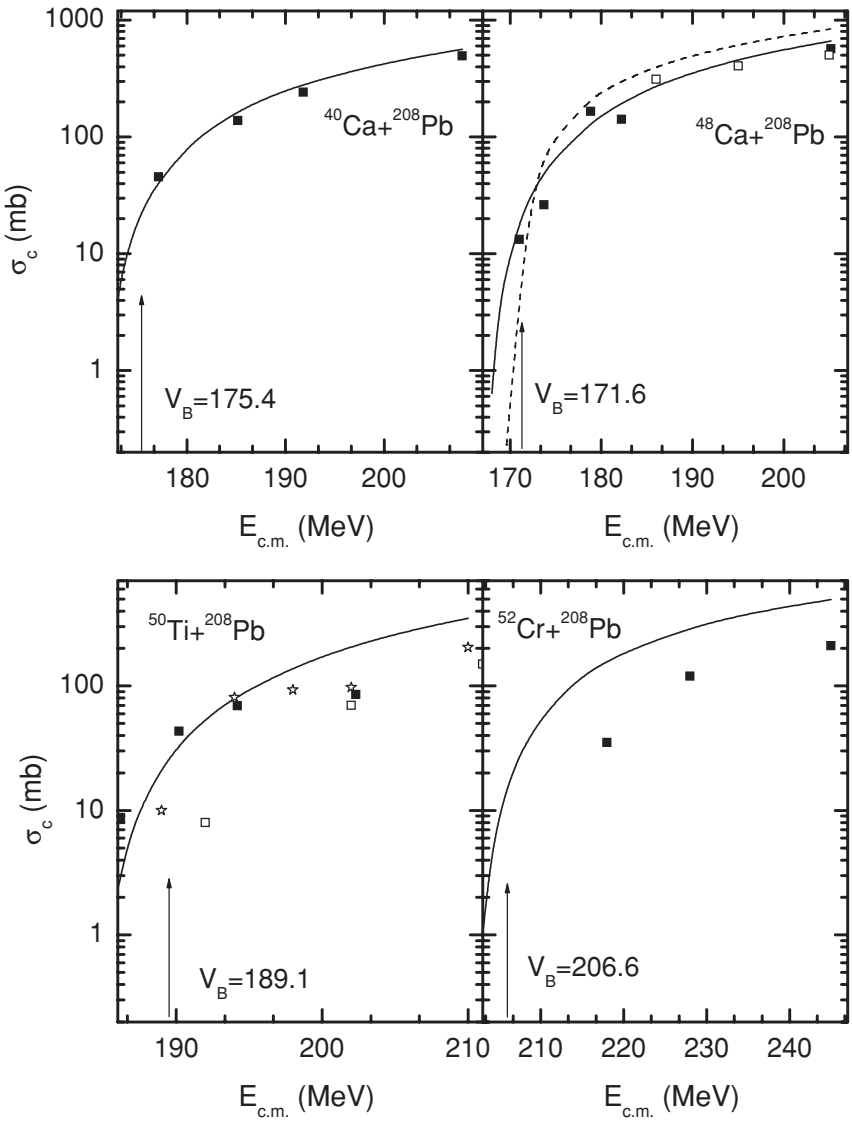

FIG. 9. Calculated capture cross sections for the indicated reactions. The experimental data for the ^{40}Ca + ^{208}Pb reaction are borrowed from Ref. [34]. The experimental data for the ^{48}Ca + ^{208}Pb reaction are borrowed from Refs. [34] (closed symbols) and [35] (open symbols). The experimental data for the ^{50}Ti + ^{208}Pb reaction are borrowed from Refs. [36] (closed squares), [29] (open squares), and [37] (star symbols). The experimental data the for ^{52}Cr + ^{208}Pb reaction are borrowed from Ref. [29]. For the ^{48}Ca + ^{208}Pb reaction, the capture cross section calculated with the Wong formula (15) is presented by the dashed curve.

about 4 MeV below the Coulomb barrier to about 70 MeV above the Coulomb barrier. The discrepancy between the theory and experiment for the ^{52}Cr + ^{208}Pb reaction can be explained as follows. The experimental capture cross section $\sigma_c^{(\mathrm{ex})}$ is the sum of quasifission σ_{qf}, fusion-fission σ_{ff}, and fusion-evaporation residue σ_{ER} cross sections. The two last cross sections σ_{ff} and σ_{ER} are quite small (because of very small fusion probability or strong fusion hindrance) for the ^{52}Cr + ^{208}Pb reaction and can be disregarded. So, the question arises how accurately the quasifission products are separated from the elastic and deep inelastic products in the experiment. The system ^{52}Cr + ^{208}Pb is hindered by the potential minimum in charge (mass) asymmetry against fast sliding to more symmetric configurations and, thus, it has a large probability to decay by the quasifission. So, the products with charge (mass) asymmetries near the entrance channel give the main contributions to the distribution of quasifission products [38]. However, it is very difficult to separate in the experiment these products from the products of elastic and deep inelastic processes. One can suppose that in Ref. [29] the contribution of quasifission products near the entrance channel was underestimated. With increasing bombarding energy and, correspondingly, the excitation energy of the entrance channel configuration the probability of transition to more symmetric configurations increases and the contribution of quasifission near the entrance channel decreases (but still remains considerable). Indeed, one can see that the difference between the theory and experiment decreases with increasing bombarding energy.

One of the main criterion of validity of the measured capture cross section is the dependence $\sigma_c E_{\mathrm{c.m.}}/(\pi R_b^2 \hbar\omega_b)$ on $(E_{\mathrm{c.m.}} - V_b)/(\hbar\omega_b)$ [39]. One can see this dependence for experimental and theoretical σ_c in Fig. 10. The entrance channel effect creates the difference in the absolute value of capture cross sections. As seen in Fig. 10, the reactions with lighter projectile has a larger value of $\sigma_c E_{\mathrm{c.m.}}/(\pi R_b^2 \hbar\omega_b)$. The reason is that the pocket of the nucleus-nucleus interaction potential is deeper and wider in these reactions. For the reactions with relatively light nuclei ^{16}O, ^{19}F, ^{26}Mg, ^{28}Si, ^{32,34,36}S, and ^{40,48}Ca, the experimental points at given $(E_{\mathrm{c.m.}} - V_b)/(\hbar\omega_b)$

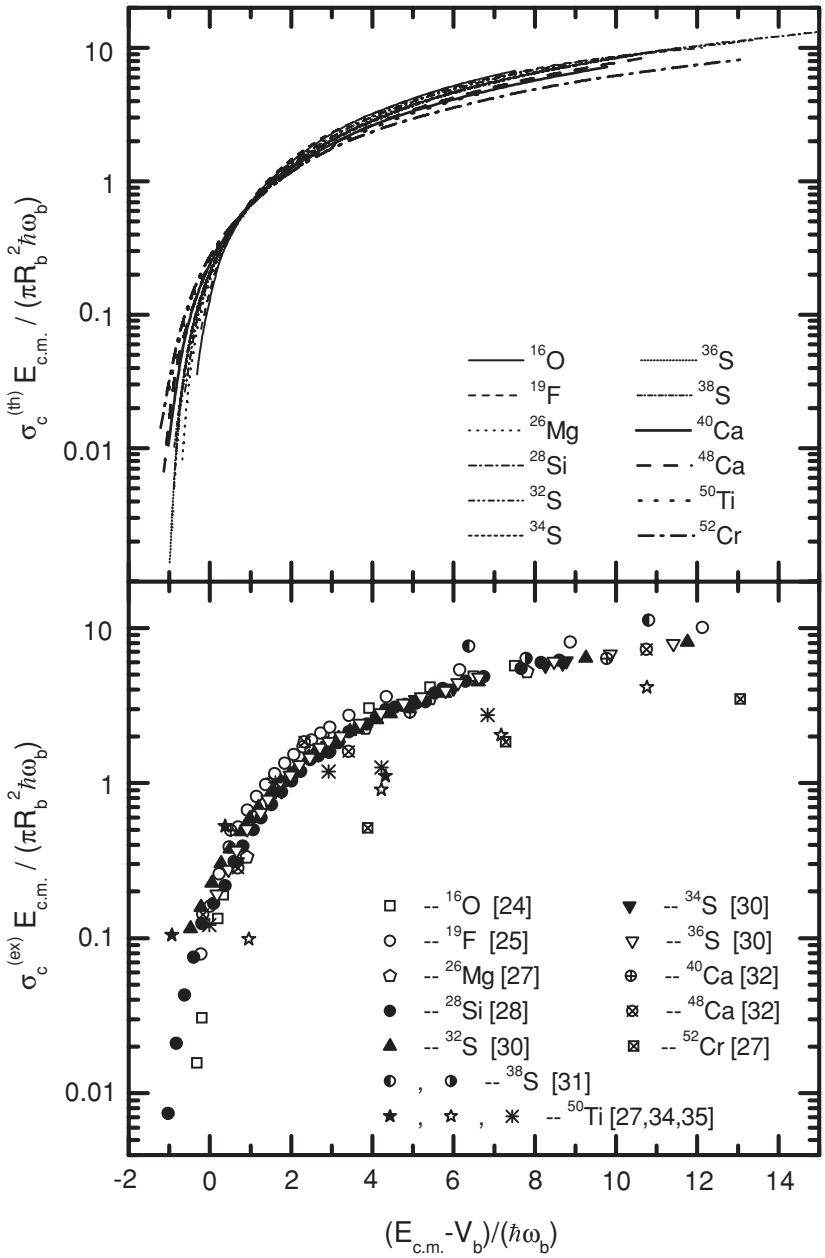

FIG. 10. The dependence of calculated (upper part) and experimental (lower part) values of $\sigma_c E_{\text{c.m.}}/(\pi R_b^2 \hbar\omega_b)$ on $(E_{\text{c.m.}} - V_b)/(\hbar\omega_b)$ for the reactions with ^{208}Pb target and various indicated projectiles. Here, $V_b = V(R = R_b, L = 0)$.

are distributed in quite narrow region. So, the dependence of $\sigma_c E_{\text{c.m.}}/(\pi R_b^2 \hbar\omega_b)$ on $(E_{\text{c.m.}} - V_b)/(\hbar\omega_b)$ seems to be universal for all reactions at $E_{\text{c.m.}} \geqslant V_b$. For comparatively heavy systems ^{50}Ti, ^{52}Cr + ^{208}Pb, where the complete fusion process is strongly suppressed but the quasifission is strongly enhanced near the entrance channel, the experimental points strongly deflect from this narrow region. As mentioned above, it can be related to the problems of the separation of quasifission near the entrance channel.

It should be noted that the experimental σ_c for the ^{52}Cr + ^{208}Pb reaction [29] can be reproduced if the static Coulomb barrier is effectively replaced with the dynamical barrier [3]. The shift of static barrier is the so-called extra-push effect. However, the experimental results on the cold fusion reactions with ^{208}Pb and ^{209}Bi targets showed that there is no extra-push effect in the entrance channel [7]. Therefore, the use of the barrier shift would underestimate the real value of σ_c.

For the reactions considered, the capture cross sections initially increase with $E_{\text{c.m.}}$ but then decrease proportionally to $1/E_{\text{c.m.}}$. In our model the capture is assumed to occur for all L values from $L = 0$ to $L = L_{\text{crit}}$ for which a pocket of nucleus-nucleus potential exists in the sticking limit. When L_{crit} becomes less then the maximal angular momentum $L_{\max}$ at given bombarding energy, the capture cross section can decrease at large $E_{\text{c.m.}}$. So there is limitation of capture due to the entrance channel effects. At $L \geqslant L_{\text{crit}}$, the sum of centrifugal and Coulomb forces overcompensates the nuclear attraction. At $L < L_{\text{crit}}$, the decay products near the entrance channel would have mainly a quasifission origin. For the reactions ^{54}Fe + ^{208}Pb and ^{58}Ni + ^{208}Pb, the capture cross section reaches the maximum value at $E_{\text{c.m.}} \approx 250$ and

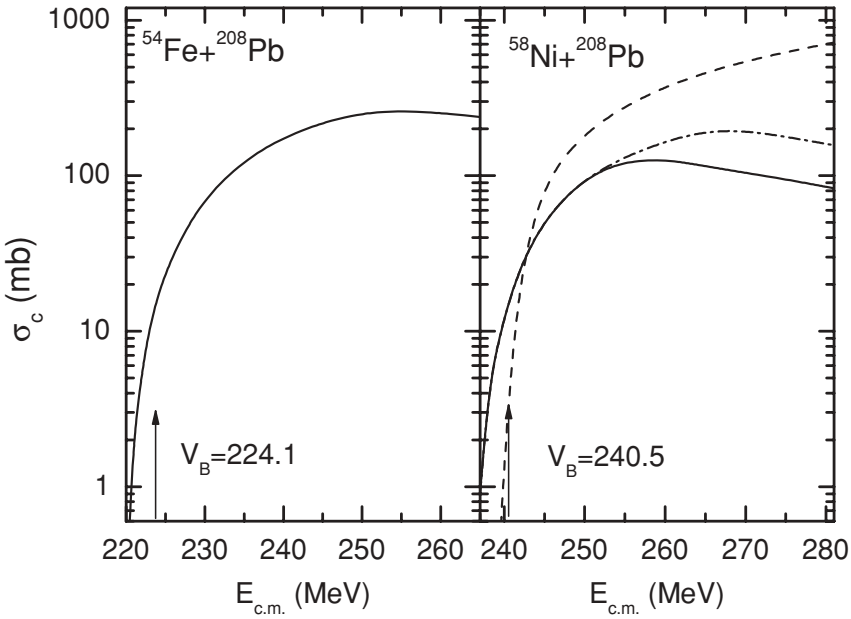

FIG. 11. Calculated capture cross sections for the $^{54}\mathrm{Fe} + ^{208}\mathrm{Pb}$ and $^{58}\mathrm{Ni} + ^{208}\mathrm{Pb}$ reactions. For the $^{58}\mathrm{Ni} + ^{208}\mathrm{Pb}$ reaction, the capture cross sections calculated with the Wong formula (15) are presented by the dashed curve. The calculated σ_c in the case of the increase of potential well depth by 0.5 MeV is presented by the dash-dotted curve.

260 MeV, respectively, i.e., at energies not far above of the Coulomb barriers (Fig. 11). The sensitivity of the position of this maximum to the depth of potential pocket is demonstrated in Fig. 11. For the $^{58}\mathrm{Ni} + ^{208}\mathrm{Pb}$ reaction, the absolute value of σ_c slightly increases and the maximum is shifted by 10 MeV toward higher energies with increasing the depth by 0.5 MeV. It will be interesting to measure such dependence of the capture cross section on bombarding energy for the $^{58}\mathrm{Ni} + ^{208}\mathrm{Pb}$ reaction. This will give us an opportunity to draw a conclusion about the depth of the potential pocket in the entrance channel. One can also answer the question whether adiabatic or diabatic regime is realized in the capture process because the potential is sensitive to that.

For the reactions $^{16}\mathrm{O}$, $^{48}\mathrm{Ca}$, $^{58}\mathrm{Ni} + ^{208}\mathrm{Pb}$, we compared our results with the capture cross sections obtained with the Wong formula [3]

$$\sigma_c(E_{\mathrm{c.m.}}) = \frac{\hbar\omega_b R_b^2}{2E_{\mathrm{c.m.}}} \ln\left\{1 + \exp\left[\frac{2\pi(E_{\mathrm{c.m.}} - V_b)}{\hbar\omega_b}\right]\right\}, \quad (15)$$

where the nucleus-nucleus interaction potential is approximated by the inverted oscillator with the frequency $\omega = \omega(R = R_b)$ at $L = 0$ and the barrier height $V_b = V(R = R_b, L = 0)$. One has to note that Eq. (15) does not impose the limitation by angular momentum. This can lead to overprediction of the capture cross section at large bombarding energies (Figs. 6, 7, 9, and 11).

Figure 12 shows the time dependence of linear entropy

$$S(t) = 1 - \mathrm{Tr}\,[\rho^2(t)] \quad (16)$$

for the $^{48}\mathrm{Ca} + ^{208}\mathrm{Pb}$ reaction at $\triangle E(0) = -2$, 5, and 15 MeV. At $\triangle E(0) = 5$ MeV the entropy has a maximum value at $t \approx 0.8\hbar$/MeV, which corresponds to the time passage over the potential barrier. When the pocket reaches the potential well, the entropy takes the minimal value. This means that the minimal and maximal values of the entropy determine the more stable and unstable points of potential energy of the system, respectively. Note that the decrease of the linear entropy is connected with the decoherence phenomenon. So, the value of decoherence increases with $E_{\mathrm{c.m.}}$.

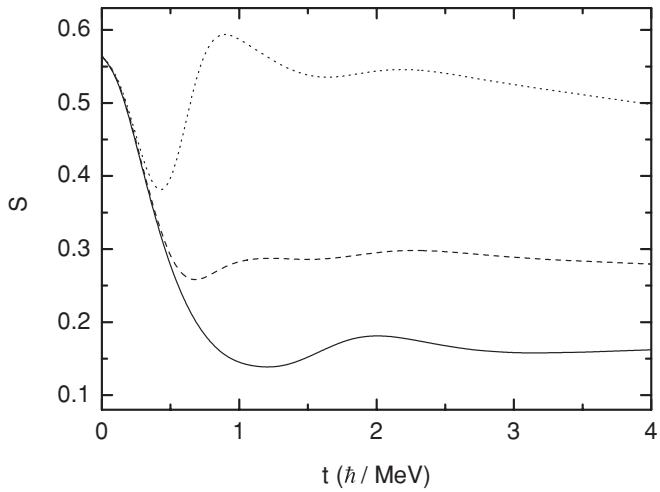

FIG. 12. The linear entropy (16) as a function of time at $\triangle E(0) = -2$ MeV (solid curve), 5 MeV (dashed curve), and 15 MeV (dotted curve).

V. SUMMARY

The reduced-density-matrix formalism has been applied for describing the process of projectile-nucleus capture by a target nucleus. The calculated capture cross sections for the reactions $^{16}\mathrm{O}$, $^{19}\mathrm{F}$, $^{26}\mathrm{Mg}$, $^{28}\mathrm{Si}$, $^{32,34,36,38}\mathrm{S}$, $^{40,48}\mathrm{Ca}$, $^{50}\mathrm{Ti} + ^{208}\mathrm{Pb}$ are in a good agreement with available experimental data. This supports the use of the formalism suggested to calculate the capture cross sections. The calculated values of σ_c strongly deviate from the experimental data in the case of the $^{52}\mathrm{Cr} + ^{208}\mathrm{Pb}$ reaction with very small (large) fusion (quasifission)

probability. We would argue that the reason creating such deviation is due to some drawback of our model but rather the system may decay by quasifission from configurations near the entrance channel that is not taken into consideration in the measurements. Note that the decay products near the entrance channel are mainly the quasifission products if $L \leqslant L_{\rm crit}$.

When the maximum angular momentum is equal to the highest trapped L wave, the capture cross section reaches the maximum value. The bombarding energy corresponding to the maximum of capture cross section decreases with increasing Coulomb repulsion ($Z_1 \times Z_2$) in the entrance channel configuration. We predict that for the ^{58}Ni + ^{208}Pb reaction the maximum of capture cross section is placed at bombarding energies about 15–25 MeV above the Coulomb barrier. The experimental verification of this effect would allow us to discriminate between adiabatic and diabatic regimes of nucleus-nucleus interaction potential and determine the depth of the potential pocket.

The universal nature of the dependence $\sigma_c E_{\rm c.m.}/(\pi R_b^2 \hbar\omega_b)$ on $(E_{\rm c.m.} - V_b)/(\hbar\omega_b)$ is shown for the heavy systems at bombarding energies $E_{\rm c.m.} \geqslant V_b$ leading to angular momenta smaller than the highest trapped L wave. Using this dependence and the calculated R_b, V_b, and $\hbar\omega_b$, one can predict the dependence of σ_c on $E_{\rm c.m.}$.

ACKNOWLEDGMENTS

This work was supported in part by DFG (Bonn) and RFBR (Moscow). The IN2P3-JINR Cooperation Programm is gratefully acknowledged.

APPENDIX

The Hamiltonian H of the total system is written as [16,21,22,40]

$$H = H_c^0 + H_b + H_{cb}, \tag{A1}$$

where H_c^0 is the Hamiltonian of the relevant collective subsystem with the pure collective potential, H_b describes the environment of the phonons, and H_{cb} describes the linear coupling between collective subsystem and environment. Eliminating the bath variables from the equations of motion of the collective subsystem and assuming the Markovian approximation for the dissipative kernel, we obtain a set of stochastic dissipative equations for harmonic (upper sign) or inverted (lower sign) oscillator

$$\begin{aligned} \dot R(t) &= \frac{P(t)}{\mu}, \\ \dot P(t) &= \mp\mu\omega^2 R(t) - \lambda_P P(t) + F_P(t), \end{aligned} \tag{A2}$$

where

$$F_P(t) = \sum_\nu F_P^\nu(t) = -\sum_\nu \alpha_\nu [f_\nu^+(t) + f_\nu(t)]$$

is the random force. Here, α_ν is real coupling constant. We identify the operators $F_P^\nu(t)$ as fluctuations because of the uncertainty in the initial conditions for the bath operators [16,19,22,40–42]. To specify the statistical properties of the fluctuations, we consider an ensemble of initial states in which the fluctuations have a Gaussian distribution with zero average value

$$\left\langle\left\langle F_P^\nu(t)\right\rangle\right\rangle = 0. \tag{A3}$$

Here, the symbol $\langle\langle \ldots \rangle\rangle$ denotes the average over the bath. To calculate the correlation functions of the fluctuations, we use the statistics

$$\begin{aligned} \langle\langle f_\nu^+(t) f_{\nu'}^+(t')\rangle\rangle &= \langle\langle f_\nu(t) f_{\nu'}(t')\rangle\rangle = 0, \\ \langle\langle f_\nu^+(t) f_{\nu'}(t')\rangle\rangle &= \delta_{\nu,\nu'} n_\nu e^{i w_\nu [t-t']}, \\ \langle\langle f_\nu(t) f_{\nu'}^+(t')\rangle\rangle &= \delta_{\nu,\nu'} (n_\nu + 1) e^{-i w_\nu [t-t']}, \end{aligned} \tag{A4}$$

where the occupation numbers for phonons depending on temperature T are given by $n_\nu = [\exp(\hbar w_\nu/T) - 1]^{-1}$ and ω_ν are the frequencies of the heat bath phonons. It is convenient to introduce the spectral density $D(w)$ of the heat bath excitations, which allows us to replace the sum over different oscillators, ν, by an integral over the frequency: $\sum_\nu \ldots \to \int_0^\infty dw D(w) \ldots$. This replacement is accompanied by the following replacements: $\alpha_\nu \to \alpha_w$, $w_\nu \to w$, $n_\nu \to n_w$. The use of the following spectral function [42]

$$D(w)\frac{|\alpha_w|^2}{\hbar w} = \frac{\lambda_P}{\pi}\frac{\gamma^2}{\gamma^2 + w^2}, \tag{A5}$$

means the Ohmic dissipation with the Lorentian cutoff (Drude dissipation) [19,41].

Using Eqs. (A2) and the solutions of Eqs. (A2),

$$\begin{aligned} R(t) &= A(t)R(0) + B(t)P(0) + \int_0^t d\tau B(\tau) F_P(t-\tau), \\ P(t) &= M(t)R(0) + N(t)P(0) + \int_0^t d\tau N(\tau) F_P(t-\tau), \end{aligned} \tag{A6}$$

where

$$\begin{aligned} A(t) &= \frac{s_2 e^{s_1 t} - s_1 e^{s_2 t}}{s_2 - s_1}, \quad B(t) = \frac{e^{s_2 t} - e^{s_1 t}}{\mu(s_2 - s_1)}, \\ M(t) &= \mp(\mu\omega)^2 B(t), \quad N(t) = \mu\dot B(t), \end{aligned}$$

and $s_1 = -\lambda_P/2 - \sqrt{\mp\omega^2 + \lambda_P^2/4}$, $s_2 = -\lambda_P/2 + \sqrt{\mp\omega^2 + \lambda_P^2/4}$ are the roots of seqular equation $s^2 + \lambda_P s \pm \omega^2 = 0$, one can obtain the equations of motion for the second moments $[\sigma_{RR}(t) = \langle R^2(t)\rangle - \langle R(t)\rangle^2, \sigma_{PP}(t) = \langle P^2(t)\rangle - \langle P(t)\rangle^2, \sigma_{RP}(t) = \frac{1}{2}\langle P(t)R(t) + R(t)P(t)\rangle - \langle P(t)\rangle\langle R(t)\rangle]$

$$\begin{aligned} \dot\sigma_{RR}(t) &= \frac{2}{\mu}\sigma_{RP}(t), \\ \dot\sigma_{PP}(t) &= -2\lambda_P\sigma_{PP}(t) \mp 2\mu\omega^2\sigma_{RP}(t) + 2D_{PP}(t), \\ \dot\sigma_{RP}(t) &= -\lambda_P\sigma_{RP}(t) \mp \mu\omega^2\sigma_{RR}(t) + \frac{1}{\mu}\sigma_{PP}(t) + 2D_{RP}(t), \end{aligned} \tag{A7}$$

with the diffusion coefficients in momentum

$$\begin{aligned} D_{PP}(t) &= \frac{1}{2}\langle P(t)F_P(t) + F_P(t)P(t)\rangle \\ &= \frac{\mu\hbar\lambda_P\gamma^2}{\pi(s_2 - s_1)}\int_0^t dt e^{-\lambda_P\tau/2}(s_2 e^{s_2\tau} - s_1 e^{s_1\tau}) \\ &\quad \times \int_0^\infty dw\ \cos(w\tau)\frac{w\coth[\hbar w/2T]}{\gamma^2 + w^2} \end{aligned} \tag{A8}$$

and in coordinate-momentum

$$D_{RP}(t) = \frac{1}{4}\langle R(t)F_P(t) + F_P(t)R(t)\rangle = \frac{\hbar\lambda_P\gamma^2}{2\pi(s_2 - s_1)}\int_0^t d\tau e^{-\lambda_P\tau/2}(e^{s_2\tau} - e^{s_1\tau}) \times \int_0^\infty dw\ \cos(w\tau)\frac{w\coth[\hbar w/2T]}{\gamma^2 + w^2}. \quad \text{(A9)}$$

Here, $\langle \ldots \rangle$ means an average over the whole system. Using the expantion $\coth[x] = 1/x + 2\sum_{k=1}^{\infty} x/(x^2 + \pi^2 k^2)$ and integrating over w and τ, we obtain from Eqs. (A8) and (A9) the explicit expressions of diffusion coefficients:

$$D_{PP}(t) = D_{PP}(\infty) + \frac{\gamma\mu\lambda_P T}{s_2 - s_1}\left(\frac{s_2(s_1-\gamma)e^{(s_2-\gamma)t} - s_1(s_2-\gamma)e^{(s_1-\gamma)t}}{\gamma(\gamma+\lambda_P) \pm \omega^2} + 2\gamma\sum_{k=1}^{\infty}\left\{\frac{\gamma\left[s_2(s_1-\gamma)e^{(s_2-\gamma)t} - s_1(s_2-\gamma)e^{(s_1-\gamma)t}\right]}{\left(\gamma^2-\nu_k^2\right)[\gamma(\gamma+\lambda_P)\pm\omega^2]} + \frac{\nu_k[s_2(s_1-\nu_k)e^{(s_2-\nu_k)t} - s_1(s_2-\nu_k)e^{(s_1-\nu_k)t}]}{\left(\nu_k^2-\gamma^2\right)[\nu_k(\nu_k+\lambda_P)\pm\omega^2]}\right\}\right), \quad \text{(A10)}$$

$$D_{RP}(t) = D_{RP}(\infty) + \frac{\gamma\lambda_P T}{s_2 - s_1}\left(\frac{(s_1-\gamma)e^{(s_2-\gamma)t} - (s_2-\gamma)e^{(s_1-\gamma)t}}{2[\gamma(\gamma+\lambda_P)\pm\omega^2]} + \gamma\sum_{k=1}^{\infty}\left\{\frac{\gamma[(s_1-\gamma)e^{(s_2-\gamma)t} - (s_2-\gamma)e^{(s_1-\gamma)t}]}{\left(\gamma^2-\nu_k^2\right)[\gamma(\gamma+\lambda_P)\pm\omega^2]} + \frac{\nu_k[(s_1-\nu_k)e^{(s_2-\nu_k)t} - (s_2-\nu_k)e^{(s_1-\nu_k)t}]}{\left(\nu_k^2-\gamma^2\right)[\nu_k(\nu_k+\lambda_P)\pm\omega^2]}\right\}\right), \quad \text{(A11)}$$

where the asymptotic diffusion coefficients $D_{PP}(\infty)$ and $D_{RP}(\infty)$ are defined by Eqs. (3) and (4), respectively. The upper (lower) sign is for the harmonic (inverted) oscillator in all expressions of this Appendix. In the case of an inverted oscillator, there is a constraint in calculating the diffusion coefficients with formulas (A10) and (A11) at low temperatures $T \leqslant T_{\rm cr} = \hbar s_2/(2\pi)$, where $T_{\rm cr}$ is the critical temperature of the transition from the regime of thermal activation to the regime of macroscopic quantum tunneling through a parabolic barrier (s_2 is a real positive root of secular equation) [13,15,18]. At $T \leqslant T_{\rm cr}$, D_{PP} and D_{RP} show no asymptotic behavior and diverge as functions of time. The reason of the difficulty at $T \leqslant T_{\rm cr}$ is that the collective subsystem becomes faster than the heat bath [13].

Using the representation of the digamma function $\psi(z) = \Gamma'(z)/\Gamma(z)$ in the infinite sum, the Eqs. (3) and (4) are written as follows:

$$D_{PP}(\infty) = -\frac{\mu T\gamma^2\lambda_P}{\gamma(\gamma+\lambda_P)\pm\omega^2} + \frac{\mu\gamma^4\hbar\lambda_P^2\psi\left(\frac{\hbar\gamma}{2\pi T}\right)}{\pi\left[(\gamma^2\pm\omega^2)^2 - \gamma^2\lambda_P^2\right]} - \frac{\mu\omega^4\gamma^2\hbar\lambda_P\psi\left(\frac{-\hbar s_2}{2\pi T}\right)}{\pi s_1(s_2-s_1)\left(s_2^2-\gamma^2\right)} - \frac{\mu\omega^4\gamma^2\hbar\lambda_P\psi\left(\frac{-\hbar s_1}{2\pi T}\right)}{\pi s_2(s_1-s_2)\left(s_1^2-\gamma^2\right)}, \quad \text{(A12)}$$

$$D_{RP}(\infty) = -\frac{T\gamma\lambda_P}{2[\gamma(\gamma+\lambda_P)\pm\omega^2]} - \frac{\gamma^2(\gamma^2\pm\omega^2)\hbar\lambda_P\psi\left(\frac{\hbar\gamma}{2\pi T}\right)}{2\pi\left[(\gamma^2\pm\omega^2)^2 - \gamma^2\lambda_P^2\right]} - \frac{\pm\omega^2\gamma^2\hbar\lambda_P\psi\left(\frac{-\hbar s_2}{2\pi T}\right)}{2\pi s_1(s_2-s_1)\left(s_2^2-\gamma^2\right)} - \frac{\pm\omega^2\gamma^2\hbar\lambda_P\psi\left(\frac{-\hbar s_1}{2\pi T}\right)}{2\pi s_2(s_1-s_2)\left(s_1^2-\gamma^2\right)}. \quad \text{(A13)}$$

For the harmonic and inverted (at $T > T_{\rm cr}$) oscillators, in the quantum regime, $\hbar\omega \gg 2T$, we have

$$D_{PP}(\infty) = \frac{\mu\gamma^2\hbar\lambda_P^2\left[s_1^2\left(s_2^2-\gamma^2\right)\ln\left(s_1^2/\gamma^2\right) + s_2^2\left(\gamma^2-s_1^2\right)\ln\left(s_2^2/\gamma^2\right)\right]}{2\pi\left(s_1^2-s_2^2\right)\left(s_1^2-\gamma^2\right)\left(s_2^2-\gamma^2\right)} + \frac{\pi\mu\lambda_P^2\gamma^4T^2\left(\lambda_P^2 \mp 2\omega^2\right)}{3\hbar\omega^4\left[\gamma^2\lambda_P^2 - (\gamma^2\pm\omega^2)^2\right]} + \delta_{-,\pm}\frac{\mu\hbar\lambda_P\gamma^2\omega^4\cot[\hbar s_2/(2T)]}{s_1^2(s_1-s_2)\left(s_2^2-\gamma^2\right)}, \quad \text{(A14)}$$

$$D_{RP}(\infty) = \frac{\gamma^2\hbar\lambda_P\left[\left(s_1^2\pm\omega^2\right)\left(\gamma^2-s_2^2\right)\ln\left(s_1^2/\gamma^2\right) + \left(s_2^2\pm\omega^2\right)\left(s_1^2-\gamma^2\right)\ln\left(s_2^2/\gamma^2\right)\right]}{4\pi\left(s_1^2-s_2^2\right)\left(s_1^2-\gamma^2\right)\left(s_2^2-\gamma^2\right)} + \frac{\pi\lambda_P T^2\left(\gamma^4\lambda_P^2 \mp \omega^2(\gamma^2\pm\omega^2)^2\right)}{6\hbar\omega^4\left[\gamma^2\lambda_P^2 - (\gamma^2\pm\omega^2)^2\right]} - \delta_{-,\pm}\frac{\hbar\lambda_P\gamma^2\omega^2\cot[\hbar s_2/(2T)]}{2s_1(s_1-s_2)\left(s_2^2-\gamma^2\right)}. \quad \text{(A15)}$$

Here, $\delta_{-,-} = 1$ and $\delta_{-,+} = 0$. At $T \geqslant 0$ for a harmonic oscillator and at $T > T_{\rm cr}$ for an inverted oscillator, the asymptotic diffusion coefficients have the finite values and satisfy the fluctuation-dissipation relation. The values of $D_{PP}(t)$ and $D_{RP}(t)$ reach their asymptotic values in time considerable shorter than the time of capture process. We start the calculation of capture probability at R where one can assume $T > T_{\rm cr} \lesssim 0.5$ MeV and, thus, the diffusion coefficients used ensure that the density matrix is positive and normalized to unity at any instant.

If $\lambda_P \ll \omega \ll \gamma$ (the Markovian and underdamped limits), the Eq. (3) leads to the well-known fluctuation-dissipation theorem [13,15,18]

$$D_{PP}(\infty) = \mu\lambda_P T^*$$

with effective temperatures $T^* = \frac{\hbar\omega}{2}\coth[\hbar\omega/(2T)]$ and $T^* = \frac{\hbar\omega}{2}\cot[\hbar\omega/(2T)]$ for the harmonic and inverted oscillators, respectively. At $\omega \ll T$ this relation leads to $D_{PP}(\infty) = \mu\lambda_P T$. At $T \to 0$, the asymptotic D_{PP} for a harmonic oscillator has the finite value: $D_{PP}(\infty) = \mu\lambda_P\frac{\hbar\omega}{2}$. In the case of an inverted oscillator, we encounter a constraint at $T \leqslant T_{\rm cr} = \hbar\omega/(2\pi)$ discussed above.

[1] V. V. Volkov, Phys. Rep. **44**, 93 (1978).
[2] W. U. Schröder and J. R. Huizenga, in *Treatise on Heavy-Ion Science*, edited by D. A. Bromley (Plenum, New York, 1984), Vol. 2, p. 115.
[3] P. Fröbrich and R. Lipperheide, *Theory of Nuclear Reactions* (Clarendon, Oxford, 1996).
[4] M. Beckerman, Rep. Prog. Phys. **51**, 1047 (1984).
[5] G. G. Adamian, A. K. Nasirov, N. V. Antonenko, and R. V. Jolos, Phys. Part. Nuclei **25**, 583 (1994).
[6] R. V. Jolos, A. I. Muminov, and A. K. Nasirov, Eur. Phys. J. A **4**, 245 (1999); G. Giardina, S. Hofmann, A. I. Muminov, and A. K. Nasirov, *ibid.* **8**, 205 (2000); G. Fazio *et al.*, *ibid.* **22**, 75 (2004).
[7] S. Hofmann and G. Münzenberg, Rev. Mod. Phys. **72**, 733 (2000).
[8] Yu. Ts. Oganessian, J. Phys. G **34**, R165 (2007).
[9] K. Morita *et al.*, J. Phys. Soc. Jpn. **73**, 2593 (2004).
[10] J. F. Liang *et al.*, Phys. Rev. C **75**, 054607 (2007); R. N. Sagaidak *et al.*, Eur. Phys. J. D **45**, 59 (2007); J. F. Liang *et al.*, Phys. Rev. Lett. **91**, 152701 (2003); A. M. Vinodkumar *et al.*, Phys. Rev. C **74**, 064612 (2006).
[11] M. Dasgupta, D. J. Hinde, N. Rowley, and A. M. Stefanini, Annu. Rev. Nucl. Part. Sci. **48**, 401 (1998).
[12] K. Washiyama, D. Lacroix, and S. Ayik, Phys. Rev. C **79**, 024609 (2009); S. Ayik, K. Washiyama, and D. Lacroix, *ibid.* **79**, 054606 (2009); S. Ayik, Phys. Lett. **B658**, 174 (2008).
[13] V. V. Sargsyan, Z. Kanokov, G. G. Adamian, and N. V. Antonenko, Phys. Rev. C **77**, 024607 (2008).
[14] P. Fröbrich, Phys. Rep. **C116**, 337 (1984).
[15] H. Hofmann, Phys. Rep. **284**, 137 (1997); H. Hofmann and D. Kiderlen, Int. J. Mod. Phys. E **7**, 243 (1998); C. Rummel and H. Hofmann, Nucl. Phys. **A727**, 24 (2003).
[16] G. G. Adamian, N. V. Antonenko, Z. Kanokov, and V. V. Sargsyan, Teor. Mat. Fiz. **145**, 87 (2005) [Theor. Math. Phys. **145**, 1443 (2006)]; Z. Kanokov, Yu. V. Palchikov, G. G. Adamian, N. V. Antonenko, and W. Scheid, Phys. Rev. E **71**, 016121 (2005); Yu. V. Palchikov, Z. Kanokov, G. G. Adamian, N. V. Antonenko, and W. Scheid, *ibid.* **71**, 016122 (2005); Sh. A. Kalandarov, Z. Kanokov, G. G. Adamian, and N. V. Antonenko, *ibid.* **74**, 011118 (2006); **75**, 031115 (2007).
[17] J. D. Bao and Y.-Z. Zhuo, Phys. Rev. C **67**, 064606 (2003).
[18] N. Takigawa, S. Ayik, K. Washiyama, and S. Kimura, Phys. Rev. C **69**, 054605 (2004); S. Ayik, B. Yilmaz, A. Gokalp, O. Yilmaz, and N. Takigawa, *ibid.* **71**, 054611 (2005); B. Yilmaz, S. Ayik, Y. Abe, and D. Boilley, Phys. Rev. E **77**, 011121 (2008).
[19] D. Zubarev, V. Morozov, and G. Röpke, *Statistical Mechanics of Nonequilibrium Processes* (Akademie Verlag, Berlin, 1997); U. Weiss, *Quantum Dissipative Systems* (World Scientific, Singapore, 1999); C. W. Gardiner, *Quantum Noise* (Springer, Berlin, 1991); N. G. van Kampen, *Stochastic Processes in Physics and Chemistry* (North-Holland, Amsterdam, 1981); H. J. Carmichael, *An Open System Approach to Quantum Optics* (Springer, Berlin, 1993).
[20] V. V. Dodonov and V. I. Man'ko, Trudy Fiz. Inst. AN **167**, 7 (1986); H. Dekker, Phys. Rep. **80**, 1 (1981); A. Isar, A. Sandulescu, H. Scutaru, E. Stefanescu, and W. Scheid, Int. J. Mod. Phys. E **3**, 635 (1994); G. G. Adamian, N. V. Antonenko, and W. Scheid, Phys. Lett. **A244**, 482 (1998); **A260**, 39 (1999); Nucl. Phys. **A645**, 376 (1999); Yu. V. Palchikov, G. G. Adamian, N. V. Antonenko, and W. Scheid, J. Phys. A **33**, 4265 (2000); Physica A **316**, 297 (2002).
[21] A. O. Caldeira and A. J. Leggett, Physica A **121**, 587 (1983); Ann. Phys. (NY) **149**, 374 (1983); Phys. Rev. Lett. **46**, 211 (1981); **48**, 1571 (1982).
[22] H. Grabert, P. Schramm, and G. L. Ingold, Phys. Rep. **168**, 115 (1988); P. Talkner, Ann. Phys. (NY) **167**, 390 (1986).
[23] V. V. Sargsyan, Yu.V. Palchikov, Z. Kanokov, G. G. Adamian, and N. V. Antonenko, Phys. Rev. A **75**, 062115 (2007); Physica A **386**, 36 (2007); Phys. Rev. C **76**, 064604 (2007).
[24] G. G. Adamian *et al.*, Int. J. Mod. Phys. E **5**, 191 (1996).
[25] V. V. Sargsyan, A. S. Zubov, Z. Kanokov, G. G. Adamian, and N. V. Antonenko, Phys. At. Nucl. **72**, 425 (2009).
[26] C. R. Morton, A. C. Berriman, M. Dasgupta, D. J. Hinde, J. C. Newton, K. Hagino, and I. J. Thompson, Phys. Rev. C **60**, 044608 (1999).
[27] D. J. Hinde, A. C. Berriman, M. Dasgupta, J. R. Leigh, J. C. Mein, C. R. Morton, and J. C. Newton, Phys. Rev. C **60**, 054602 (1999).
[28] B. B. Back *et al.*, Phys. Rev. C **32**, 195 (1985).
[29] R. Bock *et al.*, Nucl. Phys. **A388**, 334 (1982).
[30] D. J. Hinde *et al.*, Nucl. Phys. **A592**, 271 (1995).
[31] M. Dasgupta and D. J. Hinde, Nucl. Phys. **A734**, 148 (2004).
[32] D. J. Hinde, M. Dasgupta, N. Herrald, R. G. Neilson, J. C. Newton, and M. A. Lane, Phys. Rev. C **75**, 054603 (2007).
[33] W. Loveland *et al.*, Phys. Rev. C **74**, 044607 (2006).
[34] A. J. Pacheco *et al.*, Phys. Rev. C **45**, 2861 (1992).
[35] J. Toke *et al.*, Nucl. Phys. **A440**, 327 (1985).

[36] R. S. Naik *et al.*, Phys. Rev. C **76**, 054604 (2007).
[37] H.-G. Clerc *et al.*, Nucl. Phys. **A419**, 571 (1984).
[38] G. G. Adamian, N. V. Antonenko, and W. Scheid, Phys. Rev. C **68**, 034601 (2003).
[39] P. R. S. Gomes, talk at the Int. Conf. NSD09, Dubrovnik (2009); AIP Conf. Proc. 1165 (in press).
[40] F. Haake and R. Reibold, Phys. Rev. A **32**, 2462 (1985); B. L. Hu, J. P. Paz, and Y. Zhang, Phys. Rev. D **45**, 2843 (1992); R. Karrlein and H. Grabert, Phys. Rev. E **55**, 153 (1997).
[41] Yu. L. Klimontovich, *Statistical Theory of Open Systems* (Kluwer, Dordrecht, 1995); P. Hanggi, P. Talkner, and M. Borkovec, Rev. Mod. Phys. **62**, 251 (1990).
[42] K. Lindenberg and B. J. West, Phys. Rev. A **30**, 568 (1984).